



Detecting patterns of climate change in long-term forecasts of marine environmental parameters

Gianpaolo Coro, Pasquale Pagano & Anton Ellenbroek

To cite this article: Gianpaolo Coro, Pasquale Pagano & Anton Ellenbroek (2018): Detecting patterns of climate change in long-term forecasts of marine environmental parameters, International Journal of Digital Earth, DOI: [10.1080/17538947.2018.1543365](https://doi.org/10.1080/17538947.2018.1543365)

To link to this article: <https://doi.org/10.1080/17538947.2018.1543365>



© 2018 The Author(s). Published by Informa UK Limited, trading as Taylor & Francis Group



[View supplementary material](#)



Published online: 07 Nov 2018.



[Submit your article to this journal](#)



[View Crossmark data](#)

Detecting patterns of climate change in long-term forecasts of marine environmental parameters

Gianpaolo Coro ^a, Pasquale Pagano^a and Anton Ellenbroek^b

^aIstituto di Scienza e Tecnologie dell'Informazione "A. Faedo" – CNR, Pisa, Italy; ^bFood and Agriculture Organization of the United Nations (FAO), Rome, Italy

ABSTRACT

Forecasting environmental parameters in the distant future requires complex modelling and large computational resources. Due to the sensitivity and complexity of forecast models, long-term parameter forecasts (e.g. up to 2100) are uncommon and only produced by a few organisations, in heterogeneous formats and based on different assumptions of greenhouse gases emissions. However, data mining techniques can be used to coerce the data to a uniform time and spatial representation, which facilitates their use in many applications. In this paper, streams of big data coming from AquaMaps and NASA collections of 126 long-term forecasts of nine types of environmental parameters are processed through a cloud computing platform in order to (i) standardise and harmonise the data representations, (ii) produce intermediate scenarios and new informative parameters, and (iii) align all sets on a common time and spatial resolution. Time series cross-correlation applied to these aligned datasets reveals patterns of climate change and similarities between parameter trends in 10 marine areas. Our results highlight that (i) the Mediterranean Sea may have a standalone 'response' to climate change with respect to other areas, (ii) the Poles are most representative of global forecasted change, and (iii) the trends are generally alarming for most oceans.

ARTICLE HISTORY


Received 6 July 2018
Accepted 29 October 2018


KEYWORDS

Climate change;
environmental parameters
forecasting; environmental
parameters; time series;
ecological modelling; species
distribution modelling;
AquaMaps; NASA Earth
Exchange

1. Introduction

Among the disruptive effects of climate change, ecological changes are particularly feared and monitored, also because of their influence on many aspects of human life (Fritze et al. 2008; Boon et al. 2011; Keim 2011; Sauerborn and Ebi 2012; Schleussner et al. 2016). Climate change can seriously affect species' habitat distribution especially if coupled with anthropogenic pressure (Secretariat of the Convention on Biological Diversity 2009). In several ocean areas this combination has already demonstrated its negative effects at species abundance and biodiversity levels (Cheung et al. 2009). Another consequence is the irreversible impact on a wide range of ecosystem services that are essential for human well-being, e.g. food provisioning, water quality regulation, leisure, and recreation (Harley et al. 2006). The potential impact of climate change on species' habitat distribution has also been investigated through ecological models relying on predictions of future environmental conditions. The forecasted environmental parameters are the base of several studies on ecosystems response to perturbations and habitats shift

CONTACT Gianpaolo Coro  coro@isti.cnr.it

 Supplemental data for this article can be accessed at <http://dx.doi.org/10.1080/17538947.2018.1543365>

© 2018 The Author(s). Published by Informa UK Limited, trading as Taylor & Francis Group
This is an Open Access article distributed under the terms of the Creative Commons Attribution-NonCommercial-NoDerivatives License (<http://creativecommons.org/licenses/by-nc-nd/4.0/>), which permits non-commercial re-use, distribution, and reproduction in any medium, provided the original work is properly cited, and is not altered, transformed, or built upon in any way.

(Scheffer et al. 2001; Thrush et al. 2009; Coro et al. 2016). However, reliable forecasts are mostly limited to the near future and regional levels, because of the complex modelling and high computational resources required. A high-quality forecast model for marine-related environmental parameters usually includes air and ocean currents dynamics, socio-economic human-related factors, and alternative scenarios of emissions/concentration of greenhouse gases. The required computational capabilities usually involve costly high-performance computing systems that require even weeks of computations to produce a 10-year forecast of one parameter at the regional scale (Artale et al. 2010; Gualdi et al. 2013). As a consequence, parameters forecasts in the distant-future (e.g. reaching 2100) are uncommon and published by few organisations that can afford the costs and own the required competences. These forecasts usually assume coarse hydrodynamic approximations (e.g. general circulation models), start from heterogeneous assumptions, and use different parameters, which makes them difficult to compare. Nevertheless, they represent the fundamental source of information for further data mining processes and expert analyses that detect patterns independent of the coarse approximations used by the models. These pattern recognition techniques can reveal trends of ecological change, habitat shifts, impact on fisheries, and food provisioning due to climate change. Indeed, many works have analysed the results of long-term environmental forecasts, especially at regional level (Otto et al. 2016; Uhe et al. 2016). Several of these identify temperature as a major indicator of climate change, and most forecasts estimate an increase up to 2°C in 2100 (Meinshausen et al. 2009; Schrier et al. 2013; Assessment 2018). Other works consider several parameters combined (e.g. energy, land, water, and oceans) in visual analyses enriched with standard statistics and expert discussion about possible interactions between these parameters (Biol 2008; Goldman, Kessler, and Danter 2010; Krey 2014). Most current approaches rely on the results of one or a few specific models and evaluate a model's accuracy based on the measure of how this can recreate past scenarios (Donner et al. 2011). Another use of environmental parameter forecasts is in ecological niche modelling, where the correlations between environmental conditions and a species' occurrences in its native habitat are estimated (Pearson 2007). Using forecasts, niche models can be projected in the future, for example, to extract patterns of habitat shift due to climate change out of many species habitats distributions (Coro, Pagano, and Ellenbroek 2014, 2016). In fact, pattern recognition techniques are better suited to process the output of many models, in order to overcome model-specific biases and use complementary properties of the models (Coro et al. 2018).

In this paper, AquaMaps and NASA data collections were used, which include most available and relevant long-term forecasts of environmental parameters. Altogether, these collectors publish forecasts for 9 types of environmental parameters between 1950 and 2100, at different spatial and temporal resolutions and under different socio-economic and greenhouse gases emission scenarios (IPCC SRES A2, RCP 4.5, and RCP 8.5). Based on these data, this paper presents an analysis of 126 forecast models and the process to standardise and align the data on a common spatio-temporal grid. Further, two additional variables were estimated as the difference between air and sea temperature under two distinct greenhouse gases concentration scenarios. Our analysis is oriented to marine environment, since our aim was to produce the base data for a forecast of potential climate change impact on fisheries and species distributions, and thus most variables are marine-related. In particular, 10 marine areas were selected in order to highlight the trends of the parameters in these areas and to trace similarities in the areas' response to climate change. These similarities were first qualitatively estimated through visual comparison of maps and of averaged time series, and then quantitatively inspected through time series cross-correlation analysis. The streams of big data coming from the two collections were processed through a cloud computing platform and published Open Access under standard representation formats. Also, the conversion and publication processes were openly published under a standard for computations representation.

The analysed data use different hypotheses of greenhouse gases emission scenarios. In particular, AquaMaps uses the Intergovernmental Panel on Climate Change (IPCC) Special Report on

Emissions Scenarios (SRES) – A2 scenario, which describes a heterogeneous future where independent, self-reliant nations operate in the context of a constantly increasing population, with a regionally oriented economic development, slow and fragmented technological change, and no barriers to the use of nuclear energy. Instead, NASA uses two different greenhouse gases concentration hypotheses: Representative Concentration Pathways (RCP) 4.5, a medium-concentration scenario in which total radiative forcing stabilises just after 2100 without overstepping the target level, and RCP 8.5, a high-concentration scenario due to increasing greenhouse gases emission over time.

This paper is organised as follows: Section 2 explains the data and the used computational tools and analysis techniques. Section 3 reports qualitative and quantitative comparisons and results. Section 4 discusses the compliance of our findings with other studies. Section 5 describes possible applications and reuse of our tools and analysis, and draws the conclusions.

2. Material and methods

2.1. Data and resources

Good quality annual forecasts are published by the AquaMaps Consortium for years 1950 (backwards forecast), 2050, and 2100 for 6 marine environmental parameters at 0.5° resolution: Sea surface temperature (SST), primary production, temperature at sea bottom level (SBT), sea surface salinity (SSS), salinity at sea bottom level (SBS), and ice concentration. The real observations in 2016 of these parameters come from heterogeneous data providers (Table 1), i.e. the World Ocean Atlas, NOAA Climatology, Sea Around Us, and the US National Snow and Ice Data Centres. AquaMaps uses the IPSL general circulation earth system model for the 5th IPCC report (IPSL-CM5) (Dufresne et al. 2013) to project data in 1950, 1999, 2050, and 2100 according to the IPCC

Table 1. List of parameters involved in our analysis with associated primary sources, data collectors, used approach to forecast real observations in the past and in the future, spatial and temporal resolutions, and temporal frames of the forecasts.

Parameter	Primary source	Data collector	Forecast approach	Spatial resolution (degrees)	Time resolution	Time frames
Ice concentration	US National Snow and Ice Data Centre (NSIDC)	AquaMaps	IPSL – IPCC SRES A2	0.5	Annual	1950, 2050, 2100
Temperature at sea bottom level	World Ocean Atlas	AquaMaps	IPSL – IPCC SRES A2	0.5	Annual	1950, 2050, 2100
Sea surface temperature	NOAA-NCEP Climatology	AquaMaps	IPSL – IPCC SRES A2	0.5	Annual	1950, 2050, 2100
Sea surface salinity	World Ocean Atlas	AquaMaps	IPSL – IPCC SRES A2	0.5	Annual	1950, 2050, 2100
Salinity at sea bottom level	World Ocean Atlas	AquaMaps	IPSL – IPCC SRES A2	0.5	Annual	1950, 2050, 2100
Primary production	Sea Around Us	AquaMaps	IPSL – IPCC SRES A2	0.5	Annual	1950, 2050, 2100
Minimum air temperature in RCP 4.5	CMIP5	NASA	BCSD-GCM	0.25	Daily	1950–2100
Maximum air temperature in RCP 4.5	CMIP5	NASA	BCSD-GCM	0.25	Daily	1950–2100
Precipitation in RCP 4.5	CMIP5	NASA	BCSD-GCM	0.25	Daily	1950–2100
Minimum air temperature in RCP 8.5	CMIP5	NASA	BCSD-GCM	0.25	Daily	1950–2100
Maximum air temperature in RCP 8.5	CMIP5	NASA	BCSD-GCM	0.25	Daily	1950–2100
Precipitation in RCP 8.5	CMIP5	NASA	BCSD-GCM	0.25	Daily	1950–2100

Notes: CMIP5 indicates 20 real-valued models collected by NASA from the Coupled Model Intercomparison Project Phase 5. IPSL – IPCC SRES A2 indicates use of the IPSL model to project data under the IPCC SRES A2 scenario. BCSD-GCM indicates bias-correction spatial disaggregation applied by NASA to general circulation models results.

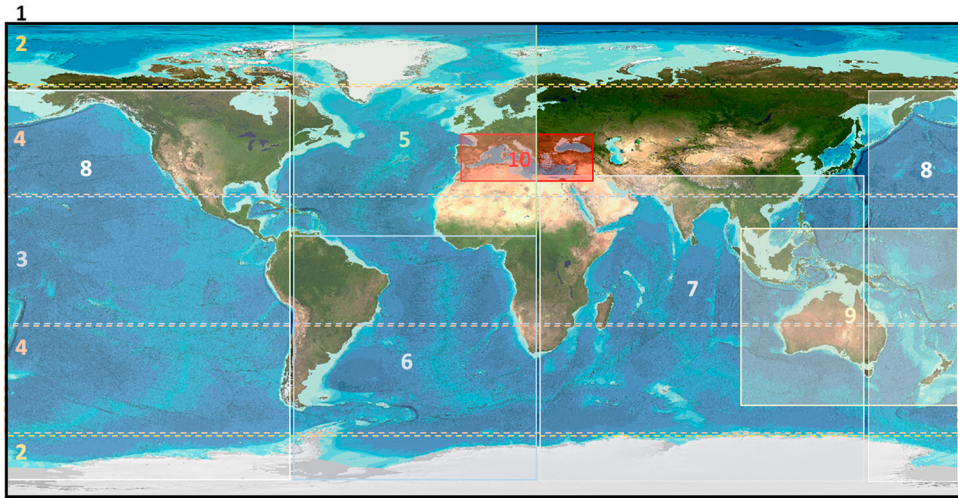


Figure 1. Bounding boxes of the ten marine areas used to detect similarities in their response to climate change: 1 (overall image outline) – Global oceans, 2 (dashed outlines) – Poles, 3 (dashed outline) – Equator, 4 (dashed outlines) – Tropics, 5 (solid outline) – North Atlantic Ocean, 6 (solid outline) – South Atlantic Ocean, 7 (solid outline) – Indian Ocean, 8 (solid outlines) – Pacific Ocean, 9 (solid outline) – Oceania and Indonesia, and 10 (solid outline) – Mediterranean Sea.

SRES A2 scenario. The values of this model are adjusted using real observations to obtain definitive values. In particular, final estimates for 2050 are obtained as

$$\begin{aligned} \text{Parameter Value in 2050} &= \text{IPSL value in 2050} \\ &+ (\text{Observation value in 2016} - \text{IPSL value in 1999}) \end{aligned}$$

The same approach is used to produce definitive data for 2100 and 1950. In the formula, the differences between real observations and modelled values in 1999 are used as a correction term that takes into account the slopes of parameter changes in each 0.5° location. As a consequence, this approach cannot produce definitive values for 1999.

The AquaMaps data have ~ 1 GB size and are distributed in unstructured textual format through the provider's Web site (www.aquamaps.org/main/envt_data.php). Metadata are available at a separate location in MS-Excel format (www.aquamaps.org/main/files/HCAFMetadata_v6.xls). Thus, processing is usually required to use these data in ecological models. Based on these parameters, AquaMaps has built effective ecological niche models that incorporate scientific expert knowledge to account for known biases and limitations of marine species occurrence records collections (Ready et al. 2010). These models use bio-climatic parameters envelopes and allow exploring geographic shifts as a response to climate change. In particular, the algorithms can estimate the distribution of a species in its native habitat today (AquaMaps-Native), in 2050 (AquaMaps-Native 2050), and in 2100 (AquaMaps-Native 2100). The 2050 and 2100 algorithms use the forecasts of their corresponding years parameters and also account for modifications in the water surface level.

NASA publishes long-term daily forecasts from 1950 to 2100 through its Earth Exchange platform (NEX-GDDP, nex.nasa.gov) at 0.25° resolution for minimum and maximum near-surface air temperature, and precipitation at surface (Table 1). Forecasts come from 20 real-valued (plus one binary) weather models provided by the Coupled Model Intercomparison Project Phase 5 (pcmdi.llnl.gov/mips/cmip5). These are general circulation models that use alternative hypotheses of medium mitigation and high concentration of greenhouse gases, corresponding to RCP 4.5 and 8.5 (Thrasher and Nemani 2015). A total of 120 real-valued models is published by NASA for the three variables in the two pathways. They are accessible through a cloud catalogue

(dataserver.nccs.nasa.gov/thredds/catalog/bypass/NEX-GDDP/catalog.html) under the Network Common Data Form standard (NetCDF) that also embeds metadata (Domenico 2011). NASA forecasts (~200 GB size) are usually post-processed before being used in ecological models, because distant-future daily estimates are not useful in long-term modelling (Hunsaker et al. 1990; Pickett et al. 2015).

2.2. Computational platform

Our experiment required analysing hundreds of gigabytes of data, thus a cloud computing platform was used to speed processing up. In particular, the DataMiner open-source system (Coro et al. 2015, 2017, freely accessible and usable after registration at services.d4science.org/group/biodiversitylab/data-miner) was used for big data preparation and processing. Using a Map-Reduce approach, DataMiner allowed our processes to parallelise files downloading and processing on a network of 30 multi-core machines (Ubuntu 14.04.5 LTS x86 64 with 16 virtual CPUs, 16 GB of random access memory, 100 GB of disk) and allowed producing maps, time series, and cross-correlations. DataMiner interoperates with the services of the D4Science distributed e-Infrastructure (Candela, Castelli, and Pagano 2009) that provides collaborative experimentation spaces supporting the exchange of the complete set of experimental parameters, inputs, and results (i.e. the computational provenance). Further, D4Science adds open-source and free-to-use Web services to publish and access the produced results either openly or tailored for a domain-focussed group of people (i.e. a Virtual Research Environment). The data produced for this paper were published Open Access on the D4Science catalogue and geospatial services (services.d4science.org/catalogue and thredds.d4science.org/thredds/catalog/public/netcdf/ClimateChange/catalog.html) as freely re-usable and distributable data. Files and results were also published in a free-access human-readable format on a D4Science high-availability storage system (CNR 2018). The cloud computing processes that operate the conversions of the AquaMaps and NASA files were developed in R and published as-a-service under the Web Processing Service (WPS) standard, which standardises their input, output, and metadata and thus is readable by GIS tools (e.g. QGIS, www.qgis.org, and ArcGIS, www.arcgis.com) and metadata catalogues (e.g. GeoNetwork, geonetwork-opensource.org, and CKAN, ckan.org). This approach is compliant with Open Science (Hey, Tansley, and Tolle 2009) by ensuring (i) the persistence of processes and data, (ii) their reusability in other experiments, and (iii) the reproducibility of the results reported in this paper.

2.3. Data preparation

The six AquaMaps environmental parameters time series were processed to produce structured and standard representation as NetCDF files, via R-based algorithms using a Map-Reduce approach through DataMiner. These custom algorithms transformed textual data into NetCDF files and published the output on the D4Science catalogue services. In particular, a Unidata-Thredds service instance (Caron and Davis 2006) enables access to the files remotely through protocols of the Open Geospatial Consortium. After standardisation, 0.5° resolution time series were available for the six AquaMaps parameters for the reference years 1950, 2050, and 2100. A 2016 scenario was generated by processing real observations in 2016 to make them consistent with the other scenarios: for each variable, real data were point-by-point automatically checked and forced to be inside upper and lower boundaries represented by the values in 1950 and in 2050. Points with increasing trend had 1950 values as lower-bounds and 2050 as upper-bounds; vice-versa for points with decreasing trend. Finally, under the approximation of linear shifting for short periods (Thrasher and Nemani 2015), a 1999 scenario was generated through a point-by-point backward linear interpolation from 2016 with slopes calculated based on the differences between the IPSL-estimated 2050 and 1999 values.

In summary, the implemented transformation process went through the following steps for each variable:

- (1) configure reference system dimensions (time, depth, longitude, and latitude) and size;
- (2) declare the dependencies of the variable from these dimensions;
- (3) extract variable's metadata from the AquaMaps reference files, e.g. size, description, data provider, etc.
- (4) make metadata compliant with the NetCDF Climate and Forecast conventions (Eaton et al. 2011);
- (5) create the file structure in the NetCDF Common Data Language (CDL);
- (6) extract definitive parameters values for 1950, 2050, and 2100 from the AquaMaps raw data;
- (7) extract IPSL-estimated values for 1950, 1999, 2050, and 2100, and real observations from the AquaMaps raw files;
- (8) produce a 2016 scenario through point-by-point consistency check of real observations with respect to 1950 and 2050;
- (9) produce a 1999 scenario through backwards linear interpolation from 2016, using the 1999 and 2050 IPSL-estimated values to calculate point-by-point slopes;
- (10) attach the payloads to the NetCDF structure and produce the file.

This workflow was executed by one different DataMiner machine for each variable using multi-core processing on each machine (Map phase) and eventually all the NetCDF files were collected, merged, and transferred to the D4Science Thredds service, with their metadata indexed on the D4Science catalogue (Reduce phase). As a result, one NetCDF file containing the 6 AquaMaps variables was produced, which contains 0.5° resolution grids of annual forecasts in the years 1950, 1999, 2016, 2050, and 2100.

Our analysis required consistent data sets from both AquaMaps and NASA aligned in time and space. Thus, AquaMaps data impose constraints on the NASA data, because they have lower resolution (0.5° vs. 0.25°) and annual estimations on five years (instead of daily reports for all years up to 2100). Further, in order to simplify the management and the analysis of the NASA data, the 20 NASA-collected models were merged into one time series for each parameter and RCP scenario. Thus, 6 merged time series (i.e. for 3 parameters and 2 RCP scenarios) were obtained by averaging the daily forecasts of all the 20 models, using an approach adopted also by NASA to produce compact representations of parameters time series (NASA-NEX 2014). In order to further compress this information, the minimum and maximum air temperature time series were averaged to obtain one temperature time series (indicated simply as SAT in the rest of the paper).

The NASA data transformation workflow went through the following steps:

- (1) download the 20 daily forecasts for each of the 3 variables in the two RCP scenarios (120 geospatial time series overall);
- (2) produce annual averages for each time series;
- (3) average the 20 annual forecasts and obtain one time series for each variable and RCP scenario (6 time series overall);
- (4) average the minimum and maximum air temperature time series and obtain one averaged air temperature time series for each RCP scenario;
- (5) reorder the latitudes between -180 and 180 in compliance with the AquaMaps representation;
- (6) select values in 1950, 1999, 2016, 2050, and 2100 for each time series;
- (7) produce one NetCDF file for each variable and RCP scenario that follows the CF conventions for metadata descriptions.

The workflow was executed by one different DataMiner machine for each NASA model (Map phase) and eventually all the NetCDF files were collected, merged, and transferred to the D4Science

Thredds service, with their metadata indexed on the D4Science catalogue (Reduce phase). In the end, 4 annual time series (and files) with 5 years were obtained out of the NASA data, containing averaged air temperature (SAT) and precipitation in RCP 4.5 and in RCP 8.5.

2.4. Data processing

2.4.1. Estimate of two additional parameters

Two additional parameters were estimated as the differences between averaged annual near-surface air temperature and sea surface temperature (SAT-SST) in RCP 4.5 and in RCP 8.5. Although the IPCC and RCP scenarios have different geneses, these two environmental parameters are useful to highlight properties of the modulations of air temperature with respect to the same reference sea temperature. Further, these modulations are correlated with sea level variation (Bintanja, van de Wal, and Oerlemans 2005) and thus contain interesting information. Indeed, a small temperature difference between sea and air may indicate that there is no layer (e.g. ice) isolating air from the sea. The importance of the two new parameters will be clarified by the analysis reported in the next section, since they are able to highlight the differences between the responses of different marine areas to climate change better than other parameters.

2.4.2. Time series per marine area

Similar to other ocean circulation experiments (NOAA-WOCE 2002), ten marine areas were selected to detect similarities in their response to climate change (Figure 1; numerical definitions of the bounding boxes are available in supplementary material): Global oceans, Poles, Equator, Tropics, North Atlantic Ocean, South Atlantic Ocean, Indian Ocean, Pacific Ocean, Oceania and Indonesia, and Mediterranean Sea. Time series of all 12 environmental parameters were recalculated for each area by averaging their area-specific values in order to study their modulations and variances. Based on these time series the means of the mean values in the areas and the variance of these means were calculated. Especially the time series of the means' variances of a parameter is important to reveal if the parameter tends to uniformity over the areas: A decreasing variance indicates increasing agreement between the mean values across the areas (uniformity), whereas increasing variance indicates that the values will become overall more heterogeneous in the future (heterogeneity).

2.4.3. Time series cross-correlation

The time series recalculated over the areas were cross-correlated and the zero of the cross-correlation function was used as a similarity score between two time series (Rabiner and Gold 1975). This score indicates how much two time series have similar, opposite, or independent trends. By averaging the similarity scores of the correspondent time series of two areas, an overall area-similarity score was calculated, which can be interpreted as a measure of how similarly two areas respond to climate change. A similarity score was calculated also between pairs of parameters, by averaging their similarities over the areas. The results of these analyses were two symmetric comparison matrices, one for the areas and another one for the time series.

3. Results

3.1. Data visualisation

The transformation and publication of ~1 GB of AquaMaps data and of ~200 GB of NASA data into NetCDF files allowed publishing these data under a number of formats. Among these, the Web Map Service (WMS) allows visualising the files as interactive maps and overlaying them with other data, e.g. background Earth representations, species distribution maps, etc. D4Science provides an online visualisation tool for the data, accessible after free registration (services.d4science.org/group/

biodiversitylab/geo-visualisation). Visualisation is important to do a first qualitative assessment of the similarities between the parameters distributions in time (animations, images, and charts are available for all variables in supplementary material). In particular, increasing trend of temperature is visible for all temperature data (Figure 2(a–d)). Rapid increase of averaged air temperature is evident (Figure 2(c)), with air temperature in RCP 8.5 increasing most (Figure 2(d)). In this global view, effects like temperature increase at the poles due to ice concentration reduction are hidden by the larger increase in other areas. These aspects will be inspected and highlighted with the more detailed analysis reported in the next section. However, these variations are already visible in the global charts of the difference between air and surface temperatures (SAT-SST). Differences can be observed between SAT-SST in RCP 4.5 and SAT-SST in RCP 8.5 already by visually comparing the figures (Figure 2(e,f)). In particular, SAT-SST in RCP 8.5 decreases everywhere possibly indicating that the separation layers' thickness decreases. Instead, SAT-SST decrement in RCP 4.5 seems more marked at the Poles than elsewhere but with lower strength than in the RCP 8.5 scenario. The other parameters show various trends (images are available in supplementary material): a decreasing trend is visible for ice concentration, sea surface salinity presents local reductions (especially at the Poles, because of ice melting) and increases, sea bottom salinity remains quite stable, primary production has localised decrement, and precipitation increase in several areas (with higher increases in RCP 8.5) but show localised decreases, e.g. in the Mediterranean Sea.

3.2. Time series analysis

In order to further analyse the trends of the visual comparison, the time series of the 10 areas were used (Figure 3; the complete set of charts is available in supplementary material). This representation improves understanding of the variations of the analysed environmental parameters. For example, stability of bottom sea water temperature is visible in most areas, but an increase is evident at the Poles and in the Mediterranean Sea (Figure 3(b)). Linear and non-linear increase of air and sea temperature in all areas are evident, with the greater increase at the Poles, around the Equator, and in the Mediterranean Sea (Figure 3(a,c,d)). A high difference is visible between the SAT-SST variables: the RCP 4.5 time series indicates possible recovery of pre-industrial level in most areas except for the Poles and the North Atlantic Ocean, whereas values decrease everywhere in RCP 8.5 and thus no recovery is possible with high concentration of greenhouse gases (Figure 3(e,f)). As for the other parameters, ice concentration rapidly decreases at the Poles with non-linear trend. Decreases of sea surface salinity are more evident at the Poles, whereas a non-linear increase is visible in the South Atlantic Ocean and in the Mediterranean Sea in 2100. Bottom sea water salinity stability is confirmed. Primary production shows a global reduction with limited decreases except in the Mediterranean Sea. Similar trends are visible for precipitation, with greater reduction under RCP 8.5 and especially in the Mediterranean Sea.

The areas around the Poles reflect the global average trends and are thus overall representative of climate change (Figure 4(a,b)). The Mediterranean Sea is an exception, because it presents at least one different (e.g. SAT-SST, primary production) or even inverse (e.g. precipitation) trend compared to the other areas (Figure 4(c)). Apart from these evident cases, similarities between the areas are difficult to assess qualitatively and thus a quantitative assessment is necessary (e.g. between the Tropics and the other areas, Figure 4(d)).

The global average charts summarise the trends of the parameters and their variances, but they may flatten representation if the variance is too large (Figure 4(a)). Instead, the time series of the average mean values over the areas (Figure 5(a)) highlights global differences between the parameters and allows distinguishing variables having (i) overall linear and non-linear monotonic-increasing trend (SAT, precipitation, SST, SBT), (ii) overall monotonic-decreasing trend (primary production, SBS, ice concentration, SAT-SST in RCP 8.5), (iii) and recovering trend (SAT-SST in RCP 4.5). Additional information is given by the variances charts (Figure 5(b)). In particular, SAT and SAT-SST tend to overall uniformity whereas SST tends to heterogeneity,

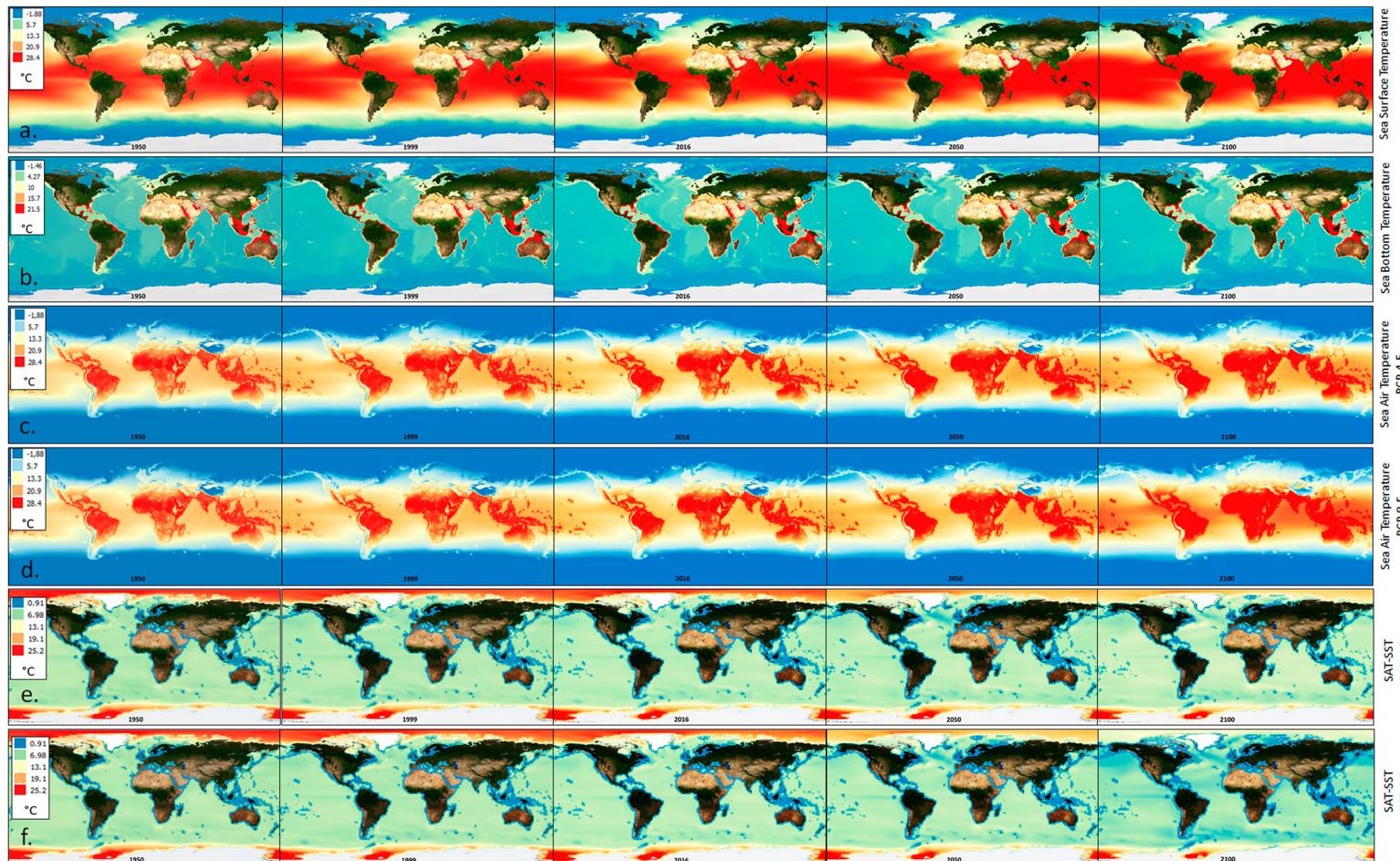


Figure 2. Representation of temperature-related time series extracted by our analysis: (a) Sea surface temperature from AquaMaps (under the IPCC SRES A2 scenario), (b) sea bottom temperature from AquaMaps (under the IPCC SRES A2 scenario), (c) averaged near-surface sea air temperature in the RCP 4.5 and (d) in the RCP 8.5 emission scenarios from NASA, (e) difference between air and sea surface temperature in the RCP 4.5 and (f) in the RCP 8.5 scenarios.

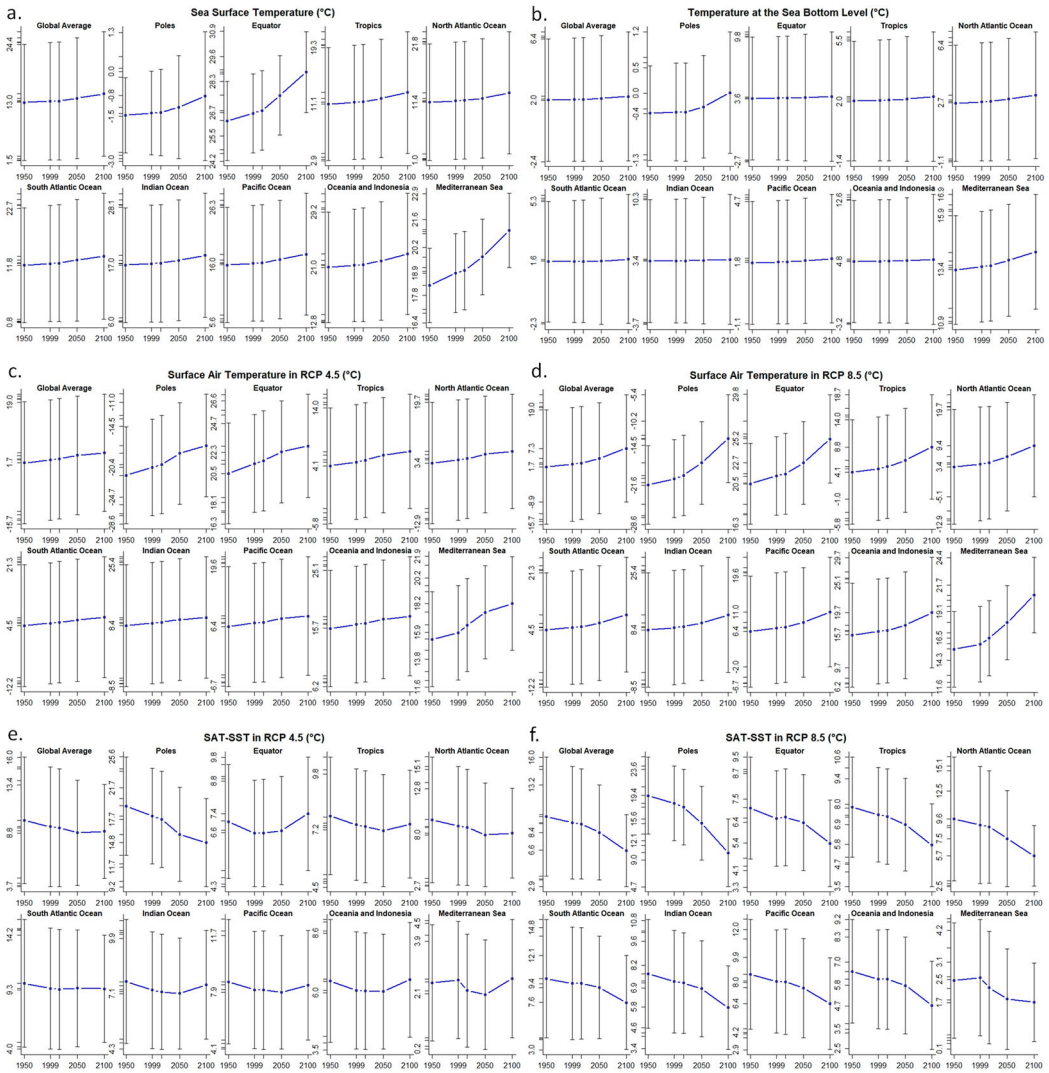


Figure 3. Charts of mean values and variances of temperature-related time series values in 10 marine areas: (a) Sea surface temperature from AquaMaps, (b) sea bottom temperature from AquaMaps, (c) averaged near-surface sea air temperature in the RCP 4.5 and (d) in the RCP 8.5 emission scenarios from NASA, (e) difference between air and sea surface temperature in the RCP 4.5 and (f) in the RCP 8.5 scenarios.

which is one important difference between air and sea surface temperatures trends. Further, the general trend of ice melting corresponds to the overall non-linear decrease of the ice concentration variance. Also, sea surface and bottom sea water salinity, bottom sea water temperature, and precipitation tend to heterogeneity across the areas, but primary production tends to uniformity.

3.3. Similarity assessment

The areas comparison matrix reveals mutual overall correlations of environmental parameters change (Table 2). These correlations can be explained as a measure of similarity between the responses of two areas to climate change. The matrix highlights that the Poles reflect global average

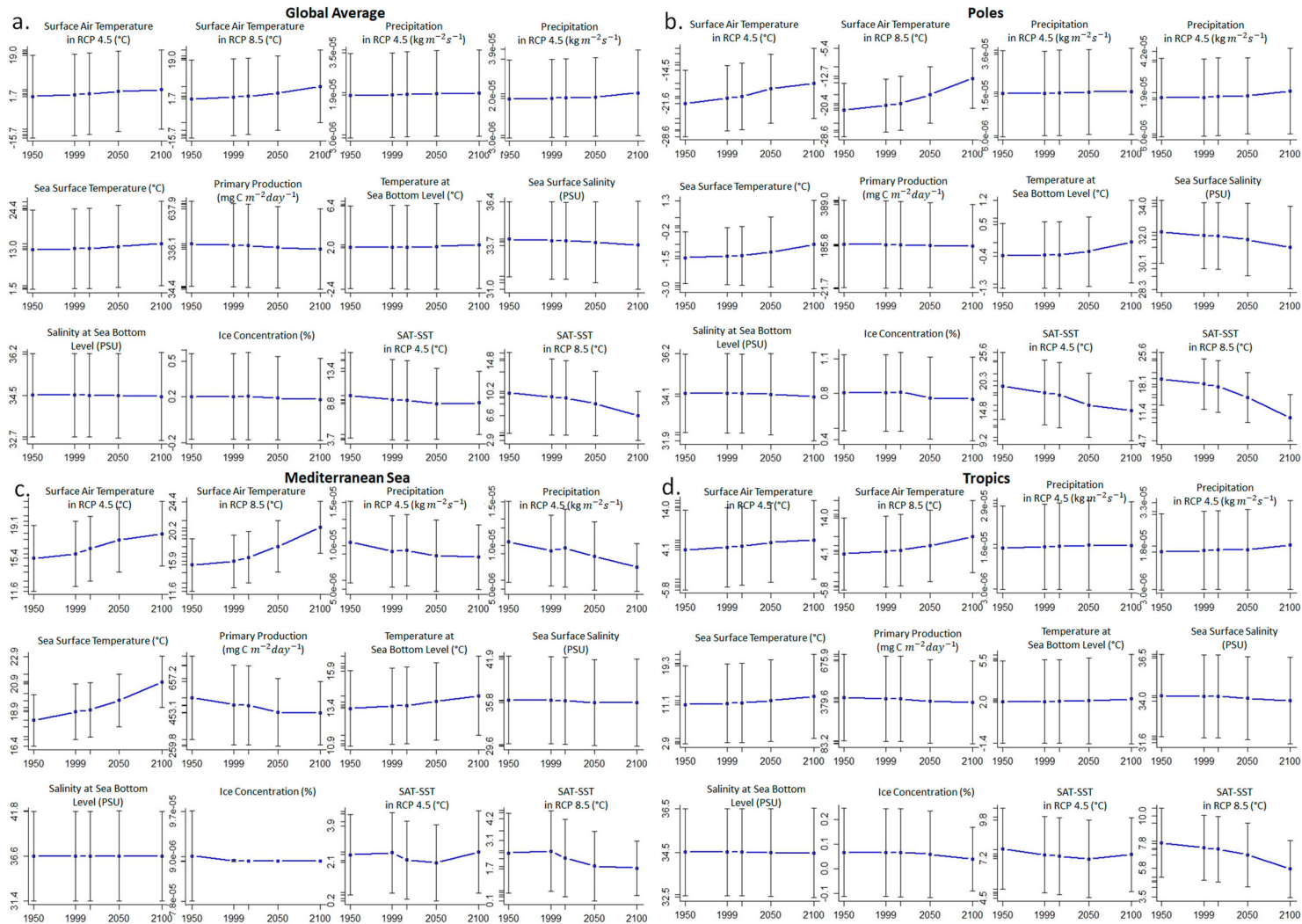


Figure 4. Charts of the average values of the 12 parameters used by our analysis in 4 of the 10 selected marine areas: (a) Global oceans, (b) Poles, (c) Mediterranean Sea, and (d) Tropics.

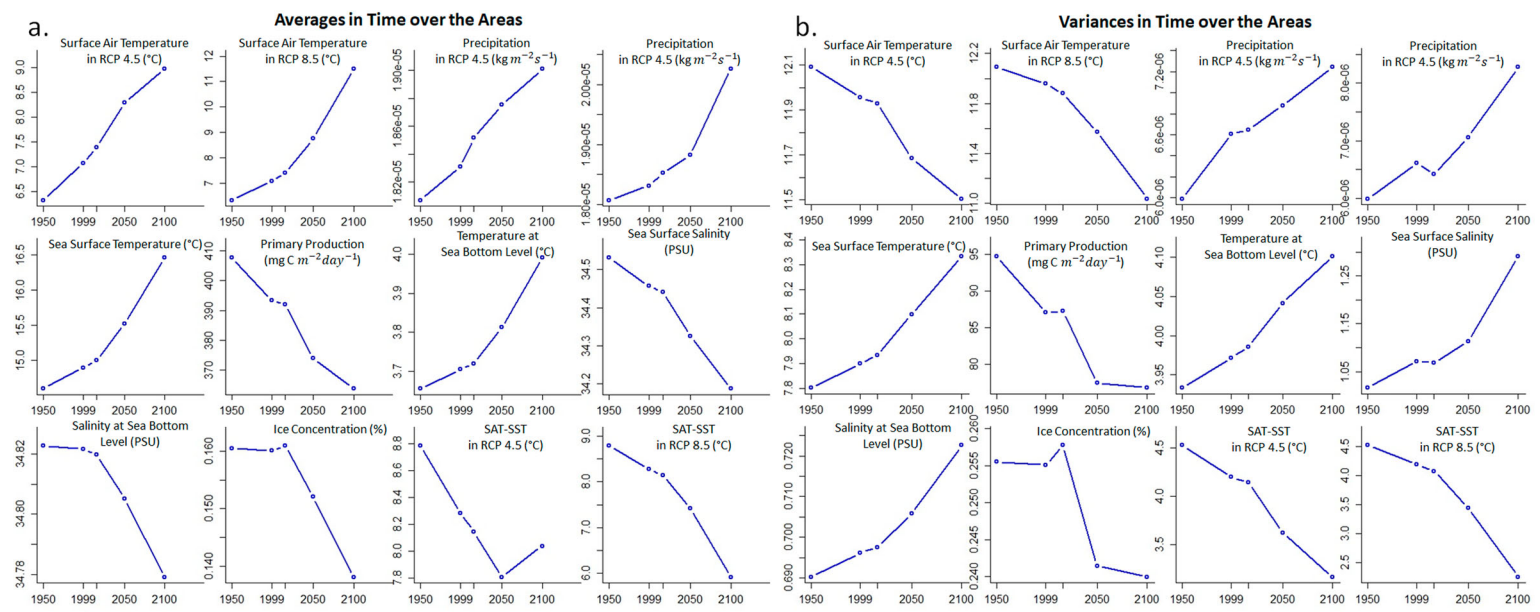


Figure 5. Charts of (a) average values and (b) variances of the 12 parameters used by our analysis, calculated over the average values of the parameters in the 10 selected marine areas.

Table 2. Matrix of the similarities between the 10 selected ocean areas, calculated as the average cross-correlation between all 12 parameters time series of the areas.

	Global Average	Poles	Equator	Tropics	North Atlantic Ocean	South Atlantic Ocean	Indian Ocean	Pacific Ocean	Oceania and Indonesia	Mediterranean Sea
Global Average	1									
Poles	0.98	1								
Equator	0.76	0.71	1							
Tropics	0.97	0.93	0.77	1						
North Atlantic Ocean	0.72	0.73	0.47	0.69	1					
South Atlantic Ocean	0.8	0.76	0.76	0.80	0.49	1				
Indian Ocean	0.95	0.90	0.82	0.98	0.63	0.80	1			
Pacific Ocean	0.96	0.91	0.82	0.99	0.64	0.80	0.99	1		
Oceania and Indonesia	0.85	0.80	0.84	0.88	0.56	0.70	0.91	0.91	1	
Mediterranean Sea	0.41	0.40	0.34	0.43	0.72	0.24	0.42	0.42	0.39	1

Note: High (over 0.9) and low (under 0.4) similarities are highlighted. Since the matrix is symmetric, specular values are not reported.

change and similar patterns exist for the Tropics and the Indian and Pacific Oceans. It also reveals the exceptional reaction of the Mediterranean Sea, which is strikingly different from the areas around the Equator, the South Atlantic Ocean, and Oceania and Indonesia. The areas around the Equator and the North and South Atlantic Oceans are neither similar between them nor with other areas; Oceania and Indonesia show a similar response to climate change as the Pacific and the Indian Oceans.

Focussing on the parameters comparison matrix, the cross-correlation analysis shows similarities between temperature parameters due to their monotonic-increasing trends everywhere (Table 3).

Table 3. Matrix of the similarities between the 12 environmental parameters used by our analysis, calculated as the average cross-correlation of the time series across the 10 selected marine areas.

	Surface Air Temperature (SAT) in RCP 4.5	Surface Air Temperature (SAT) in RCP 8.5	Precipitation in RCP 4.5	Precipitation in RCP 8.5	Sea Surface Temperature (SST)	Primary Production	Temperature at Sea Bottom Level	Sea Surface Salinity	Salinity at Sea Bottom Level	Ice Concentration	SAT-SST in RCP 4.5	SAT-SST in RCP 8.5
Surface Air Temperature (SAT) in RCP 4.5	1											
Surface Air Temperature (SAT) in RCP 8.5	0.95	1										
Precipitation in RCP 4.5	0.63	0.6	1									
Precipitation in RCP 8.5	0.57	0.63	0.85	1								
Sea Surface Temperature (SST)	0.95	1	0.59	0.62	1							
Primary Production	-0.98	-0.95	-0.63	-0.58	-0.95	1						
Temperature at Sea Bottom Level	0.93	0.99	0.56	0.62	0.99	-0.93	1					
Sea Surface Salinity	-0.71	-0.7	-0.34	-0.35	-0.7	0.71	-0.71	1				
Salinity at Sea Bottom Level	-0.75	-0.83	-0.77	-0.78	-0.82	0.76	-0.81	0.52	1			
Ice Concentration	-0.65	-0.68	-0.34	-0.43	-0.68	0.66	-0.7	0.52	0.53	1		
SAT-SST in RCP 4.5	-0.46	-0.23	-0.3	-0.08	-0.23	0.42	-0.21	0.33	0.16	0.25	1	
SAT-SST in RCP 8.5	-0.95	-0.99	-0.6	-0.64	-0.98	0.95	-0.98	0.72	0.81	0.68	0.29	1

Note: High (over 0.9) and inverse (below -0.9) similarities are highlighted. Since the matrix is symmetric, specular values are not reported.

The analysis highlights that temperatures have a strong inverse correlation with SAT-SST in RCP 8.5 due to its monotonic-decreasing trends. Precipitation has low inverse correlation with non-linearly decreasing time series like ice concentration and SAT-SST in RCP 4.5. Salinity parameters have no relevant similarity with other parameters because of non-uniform trends across the areas, e.g. correlation with ice concentration occurs at the Poles but not elsewhere (because of zero concentration), thus the correlation between these two is positive but not high.

4. Discussion

Our results agree with other studies focussing on the 12 involved environmental parameters. Increasing trends of sea surface and air temperatures related to anthropogenic climate change have been reported by many other works, along with their current and future negative effects on food provisioning and ecosystems (Ghil and Vautard 1991; Graham 1995; Liu et al. 2006; Dai 2013; Burrows et al. 2014; Chou et al. 2014; Alkama and Cescatti 2016; Alpert et al. 2016; Coro et al. 2016; Lesk, Rowhani, and Ramankutty 2016; Alexeeff et al. 2018). Further, our analysis of averages and variances across the ten areas agrees with other studies that have estimated near-future monotonic increase (with no ‘slowdown’ effect) for all temperature parameters in these areas (Karl et al. 2015; Lewandowsky et al. 2015; Dosio 2016). Our analysis also highlights that SST will have more heterogeneous values across the areas with respect to the other temperature parameters. Indeed, also other studies have reported this property and have correlated it with the influence of periodic phenomena such as the Interdecadal Pacific Oscillation and the Southern Oscillation (Kim et al. 2014; Shaltout and Omstedt 2014; Meehl et al. 2016).

The SAT-SST parameter has the property to reveal differences between the SAT and SST parameters trends, especially at the Poles. Indeed, this parameter has been recently indicated as essential in robust comparison of climate models and has been correlated with ice boundary change (Cowtan et al. 2015). As for the other environmental parameters, also other works have reported (i) non-uniform trends of salinity across the areas (Jacobs and Giulivi 2010; Lee et al. 2016), (ii) non-uniform trends in primary production with localised decrements (Brouwers and Coops 2015; Schine, van Dijken, and Arrigo 2016), and (iii) increase of precipitation at the Poles (Bintanja and Selten 2014).

The particular resilience and response of the Mediterranean Sea to climate change can be inferred after carefully analysing the results of other forecasting experiments (Adloff et al. 2015; Mariotti et al. 2015), but our analysis is able to directly highlight these peculiarities. Indeed, the rapid change that is being observed in Mediterranean marine biota is mainly due to other factors than climate change (Marbà et al. 2015).

Finally, our analysis indicates that the Poles are the most representative of global change, because their environmental parameters are going to have the highest variations. In agreement with this observation, other studies have estimated that climate change is going to have the highest impact on the Poles because of the sensitivity of polar ecosystems to sea-ice retreat and temperature increase, and poleward species migrations (Halpern et al. 2008; Doney et al. 2011).

5. Conclusions

This paper has described how currently incomparable climate change-related datasets were made uniform, and what trends can be found in and between these datasets. It has also described how data and experiments can be made available under an Open Science approach. Big data from heterogeneous sources were aligned over space and time, and were transformed into standard NetCDF files with harmonised metadata vocabularies. This operation allowed (i) extracting general properties of the data through visual comparison of maps and time series, (ii) producing variables combinations (SAT-SST) that make properties of the single parameters more evident, (iii) discovering similarities between the extracted time series, and (iv) comparing the impact of climate change between 10 different marine areas. The approach was applied to produce harmonised reference datasets for

climate change analysis for the years 1950, 1999, 2050, and 2100, along with a statistical analysis of cross-correlations between the time series.

Our analysis indicates that the expected changes at the Poles correspond to global average change. It also predicts that the Mediterranean Sea will likely have unique reaction to climate change. Introducing new parameters of sea–air temperature differences under RCP 4.5 and RCP 8.5 highlights that only under RCP 4.5 it is possible to have a recovery to pre-industrial values for this difference. Several parameters present area-specific non-linear trends and mutual inverse correlations, likely because they are naturally related to each other (e.g. sea surface salinity and ice concentration at the Poles).

The results and the processes reported in this paper are made available as free and open data sources, and we encourage further analyses. They can possibly facilitate global scale ecological models and fisheries management models. For example, our data can be used to compare species

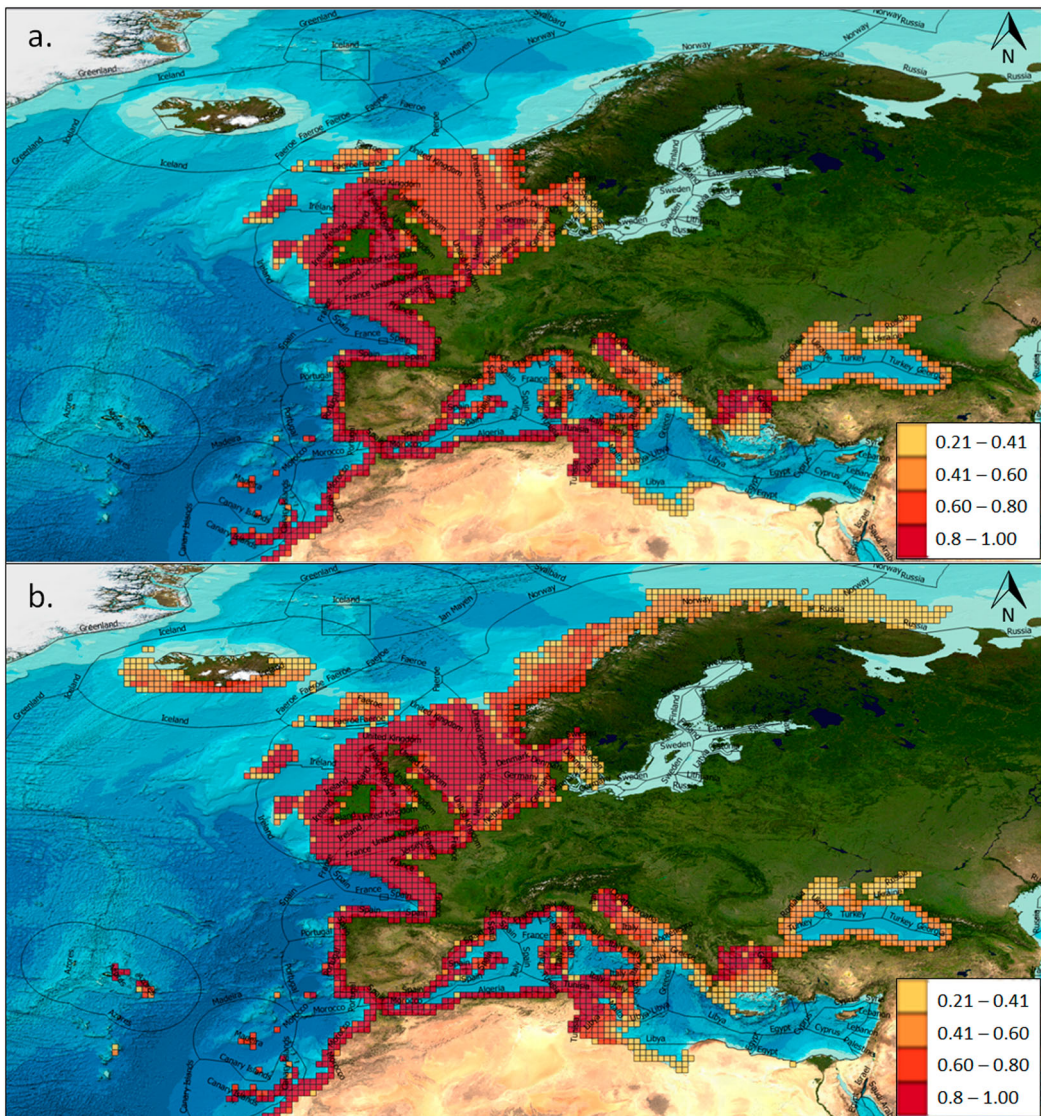


Figure 6. AquaMaps distributions of *Engraulis encrasicolus* (a) in 2016 and (b) in 2050 overlaid on Economic Exclusive Zones.

distributions today and in the future to estimate the potential impact of climate change on habitat shifts, and as a consequence on fisheries. In a yield-biomass equilibrium scenario, fish abundance in the future depends on suitable habitat distribution that changes following the effects of climate change. With our datasets, species distributions estimated for today and future years (e.g. 2050 and 2100) can be projected on Economic Exclusive Zones (EEZs) to estimate the potential impact of habitat change on EEZ-dependent fisheries (examples and images are available in supplementary material). For example, using the marine data for 2050, the AquaMaps model estimates that in 2050 the suitable habitat of the European anchovy *Engraulis encrasicolus* will increase in the North Sea, around Iceland, and in the Norwegian Sea (Figure 6). Thus, adjacent countries would likely involve this species in their future fisheries management plan. On the contrary, the suitable habitat for species like *Istiophorus platypterus* will shrink, which would have a negative impact in the Indian Ocean, Micronesia, Indonesia, and Australia. Similarly, estimated habitat loss of *Dentex angolensis* would negatively impact fisheries in Angola, Sierra Leone, Liberia, and Cameroon. Using our datasets, these distributions can be refined and other alternative models can be used with more variables and years to increase the prediction reliability.

Our analysis can also be applied to parameter projections at the regional scale (e.g. the Mediterranean Coordinated Regional Downscaling Experiment, Ruti et al. 2016). With high-resolution forecasts, the trends and similarities estimated could be added to the comparison matrix in order to refine the assessments. Our matrix can be used also in assessing the spread of invasive species due to climate change, through the analysis of similarities between the invaded and the native areas (Coro et al. 2018).

The presented experiments were feasible because an e-Infrastructure was available for data harmonisation and computationally intensive steps of the analysis. The e-Infrastructure also aided the authors in their collaboration during the experiments, and allowed publishing processes as services, and data on public online catalogues under standard representations. This enhances their re-usability in future experiments and allows reproducing and repeating all steps of our analysis, in compliance with Open Science approaches.

Disclosure statement

No potential conflict of interest was reported by the authors.

Funding

This work has received funding from the European Union's Horizon 2020 research and innovation programme under the BlueBRIDGE project [grant agreement no 675680].

ORCID

Gianpaolo Coro  <http://orcid.org/0000-0001-7232-191X>

References

- Adloff, F., S. Somot, F. Sevault, G. Jordà, R. Aznar, M. Déqué, M. Herrmann, M. Marcos, C. Dubois, E. Padorno, et al. 2015. "Mediterranean sea Response to Climate Change in an Ensemble of Twenty First Century Scenarios." *Climate Dynamics* 45 (9–10): 2775–2802.
- Alexeeff, S. E., D. Nychka, S. R. Sain, and C. Tebaldi. 2018. "Emulating Mean Patterns and Variability of Temperature Across and Within Scenarios in Anthropogenic Climate Change Experiments." *Climatic Change* 146 (3–4): 319–333.
- Alkama, R., and A. Cescatti. 2016. "Biophysical Climate Impacts of Recent Changes in Global Forest Cover." *Science* 351 (6273): 600–604.

- Alpert, A. E., A. L. Cohen, D. W. Oppo, T. M. DeCarlo, J. M. Gove, and C. W. Young. 2016. "Comparison of Equatorial Pacific Sea Surface Temperature Variability and Trends with sr/ca Records from Multiple Corals." *Paleoceanography* 31 (2): 252–265.
- Artale, V., S. Calmanti, A. Carillo, A. Dellaquila, M. Herrmann, G. Pisacane, P. M. Ruti, G. Sannino, M. V. Struglia, F. Giorgi, et al. 2010. "An Atmosphere – Ocean Regional Climate Model for the Mediterranean Area: Assessment of a Present Climate Simulation." *Climate Dynamics* 35 (5): 721–740.
- Assessment, N. C. 2018. *Summary of the Impacts of Climate Change on the United States*. <https://nca2014.globalchange.gov/>.
- Bintanja, R., and F. Selten. 2014. "Future Increases in Arctic Precipitation Linked to Local Evaporation and Sea-ice Retreat." *Nature* 509 (7501): 479.
- Bintanja, R., R. S. van de Wal, and J. Oerlemans. 2005. "Modelled Atmospheric Temperatures and Global Sea Levels Over the Past Million Years." *Nature* 437 (7055): 125.
- Birol, F. 2008. *World Energy Outlook*. Paris: International Energy Agency.
- Boon, H., L. Brown, B. Clark, P. Pagliano, K. Tsey, and K. Usher. 2011. "Schools, Climate Change and Health Promotion: A Vital Alliance." *Health Promotion Journal of Australia* 22 (4): 68–71.
- Brouwers, N., and N. Coops. 2015. *Decreasing Net Primary Production Trends in Forest and Shrub Vegetation Across Southwest Western Australia*. <http://researchrepository.murdoch.edu.au/id/eprint/32932/>.
- Burrows, M. T., D. S. Schoeman, A. J. Richardson, J. G. Molinos, A. Hoffmann, L. B. Buckley, P. J. Moore, C. J. Brown, J. F. Bruno, C. M. Duarte, et al. 2014. "Geographical Limits to Species-range Shifts Are Suggested by Climate Velocity." *Nature* 507 (7493): 492.
- Candela, L., D. Castelli, and P. Pagano. 2009. "D4science: An E-infrastructure for Supporting Virtual Research Environments." IRCDL, 166–169, Padova, Italy, January 29–30.
- Caron, J., and E. Davis. 2006. "UNIDATA's THREDDS Data Server." 22nd International Conference on Interactive Information Processing Systems for Meteorology, Oceanography, and Hydrology, Atlanta, GA, USA, January 27--February 03. Paper 10.6.
- Cheung, W. W., V. W. Lam, J. L. Sarmiento, K. Kearney, R. Watson, and D. Pauly. 2009. "Projecting Global Marine Biodiversity Impacts Under Climate Change Scenarios." *Fish and Fisheries* 10 (3): 235–251.
- Chou, S. C., A. Lyra, C. Mourão, C. Dereczynski, I. Pilotto, J. Gomes, J. Bustamante, P. Tavares, A. Silva, D. Rodrigues, et al. 2014. "Assessment of Climate Change Over South America Under Rcp 4.5 and 8.5 Downscaling Scenarios." *American Journal of Climate Change* 3 (5): 512–525.
- CNR. 2018. *Institutional Repository of Climate Change Analysis Results*. http://data.d4science.org/workspace-explorer-app?folderId=N0lmSDZHTRQSFpQUFBvJYNUtSWFJad2JnbkNCUXo4WUhnMEVxd3AvNXZ1am04L1hyVExyaGtaOEVPrk41TQ; processes source code, http://data.d4science.org/workspace-explorer-app?folderId=QThEYzA1MnVXaDcwT3ZyM3JZUWtZWGkraWZGMFdjKzQ1TzdRNFhjYVhBSnhHVy9INjE3QnUySDhjcVRZSUpSsw; and Web service endpoint, https://services.d4science.org/group/biodiversitylab/data-miner?OperatorId=org.gcube.dataanalysis.wps.statisticalmanager.synchserver.mappedclasses.transducerers.CSV_TO_NETCDF_CONVERTER_XY.
- Coro, G., L. Candela, P. Pagano, A. Italiano, and L. Liccardo. 2015. "Parallelizing the Execution of Native Data Mining Algorithms for Computational Biology." *Concurrency and Computation: Practice and Experience* 27 (17): 4630–4644.
- Coro, G., C. Magliozzi, A. Ellenbroek, K. Kaschner, and P. Pagano. 2016. "Automatic Classification of Climate Change Effects on Marine Species Distributions in 2050 Using the Aquamaps Model." *Environmental and Ecological Statistics* 23 (1): 155–180.
- Coro, G., P. Pagano, and A. Ellenbroek. 2014. "Comparing Heterogeneous Distribution Maps for Marine Species." *GIScience & Remote Sensing* 51 (5): 593–611.
- Coro, G., G. Panichi, P. Scarponi, and P. Pagano. 2017. "Cloud Computing in a Distributed E-infrastructure Using the Web Processing Service Standard." *Concurrency and Computation: Practice and Experience* 29: e4219.
- Coro, G., L. G. Vilas, C. Magliozzi, A. Ellenbroek, P. Scarponi, and P. Pagano. 2018. "Forecasting the Ongoing Invasion of Lagocephalus Sceleratus in the Mediterranean Sea." *Ecological Modelling* 371: 37–49.
- Cowtan, K., Z. Hausfather, E. Hawkins, P. Jacobs, M. E. Mann, S. K. Miller, B. A. Steinman, M. B. Stolpe, and R. G. Way. 2015. "Robust Comparison of Climate Models with Observations Using Blended Land Air and Ocean Sea Surface Temperatures." *Geophysical Research Letters* 42 (15): 6526–6534.
- Dai, A. 2013. "Increasing Drought Under Global Warming in Observations and Models." *Nature Climate Change* 3 (1): 52.
- Domenico, B. 2011. *Ogc Network Common Data form (Netcdf) Core Encoding Standard Version 1.0*. Open Geospatial Consortium Inc. Document 10, e090r3.
- Doney, S. C., M. Ruckelshaus, J. E. Duffy, J. P. Barry, F. Chan, C. A. English, H. M. Galindo, J. M. Grebmeier, A. B. Hollowed, N. Knowlton, et al. 2011. "Climate Change Impacts on Marine Ecosystems." *Annual Review of Marine Science* 4 (1): 11–37.

- Donner, L. J., B. L. Wyman, R. S. Hemler, L. W. Horowitz, Y. Ming, M. Zhao, J.-C. Golaz, P. Ginoux, S.-J. Lin, M. D. Schwarzkopf, et al. 2011. "The Dynamical Core, Physical Parameterizations, and Basic Simulation Characteristics of the Atmospheric Component am3 of the Gfdl Global Coupled Model cm3." *Journal of Climate* 24 (13): 3484–3519.
- Dosio, A. 2016. "Projections of Climate Change Indices of Temperature and Precipitation from an Ensemble of Bias-adjusted High-resolution Euro-Cordex Regional Climate Models." *Journal of Geophysical Research: Atmospheres* 121 (10): 5488–5511.
- Dufresne, J.-L., M.-A. Foujols, S. Denvil, A. Caubel, O. Marti, O. Aumont, Y. Balkanski, et al. 2013. "Climate Change Projections Using the Ipsl-cm5 Earth System Model: From Cmp3 to Cmp5." *Climate Dynamics* 40 (9): 2123–2165. doi:10.1007/s00382-012-1636-1.
- Eaton, B., J. Gregory, B. Drach, K. Taylor, S. Hankin, J. Caron, R. Signell, P. Bentley, G. Rappa, H. Höck, et al. 2011. *Netcdf Climate and Forecast (cf) Metadata Conventions Version 1.6*. cfconventions.org.
- Fritze, J. G., G. A. Blashki, S. Burke, and J. Wiseman. 2008. "Hope, Despair and Transformation: Climate Change and the Promotion of Mental Health and Wellbeing." *International Journal of Mental Health Systems* 2 (1): 13.
- Ghil, M., and R. Vautard. 1991. "Interdecadal Oscillations and the Warming Trend in Global Temperature Time Series." *Nature* 350 (6316): 324.
- Goldman, K. H., C. Kessler, and E. Danter. 2010. *Science on a Sphere*[®]. https://sos.noaa.gov/What_is_SOS/.
- Graham, N. E. 1995. "Simulation of Recent Global Temperature Trends." *Science* 267 (5198): 666–671.
- Gualdi, S., S. Somot, L. Li, V. Artale, M. Adani, A. Bellucci, A. Braun, S. Calmanti, A. Carillo, A. Dell'Aquila, et al. 2013. "The Circe Simulations: Regional Climate Change Projections with Realistic Representation of the Mediterranean Sea." *Bulletin of the American Meteorological Society* 94 (1): 65–81.
- Halpern, B. S., S. Walbridge, K. A. Selkoe, C. V. Kappel, F. Micheli, C. D'agrosa, J. F. Bruno, K. S. Casey, C. Ebert, H. E. Fox, et al. 2008. "A Global Map of Human Impact on Marine Ecosystems." *Science* 319 (5865): 948–952.
- Harley, C. D., A. Randall Hughes, K. M. Hultgren, B. G. Miner, C. J. Sorte, C. S. Thornber, L. F. Rodriguez, L. Tomanek, and S. L. Williams. 2006. "The Impacts of Climate Change in Coastal Marine Systems." *Ecology Letters* 9 (2): 228–241.
- Hey, T., S. Tansley, and K. M. Tolle. 2009. *The Fourth Paradigm: Data-Intensive Scientific Discovery*. Vol. 1. Redmond, WA: Microsoft Research.
- Hunsaker, C. T., R. L. Graham, G. W. Suter, R. V. O'Neill, L. W. Barnhouse, and R. H. Gardner. 1990. "Assessing Ecological Risk on a Regional Scale." *Environmental Management* 14 (3): 325–332.
- Jacobs, S. S., and C. F. Giulivi. 2010. "Large Multidecadal Salinity Trends Near the Pacific–Antarctic Continental Margin." *Journal of Climate* 23 (17): 4508–4524.
- Karl, T. R., A. Arguez, B. Huang, J. H. Lawrimore, J. R. McMahon, M. J. Menne, T. C. Peterson, R. S. Vose, and H.-M. Zhang. 2015. "Possible Artifacts of Data Biases in the Recent Global Surface Warming Hiatus." *Science* 348 (6242): 1469–1472.
- Keim, M. E. 2011. "Preventing Disasters: Public Health Vulnerability Reduction as a Sustainable Adaptation to Climate Change." *Disaster Medicine and Public Health Preparedness* 5 (2): 140–148.
- Kim, S. T., W. Cai, F.-F. Jin, A. Santoso, L. Wu, E. Guilyardi, and S.-I. An. 2014. "Response of el Niño sea Surface Temperature Variability to Greenhouse Warming." *Nature Climate Change* 4 (9): 786.
- Krey, V. 2014. "Global Energy-climate Scenarios and Models: A Review." *Wiley Interdisciplinary Reviews: Energy and Environment* 3 (4): 363–383.
- Lee, W., D. Li, J. M. Kaihatu, and A. Anis. 2016. "Modeling Salinity Changes in the Persian Gulf." American Geophysical Union, Ocean Sciences Meeting 2016, abstract#PO44E-3202New Orleans, Louisiana, 21–26 February, 39–44.
- Lesk, C., P. Rowhani, and N. Ramankutty. 2016. "Influence of Extreme Weather Disasters on Global Crop Production." *Nature* 529 (7584): 84.
- Lewandowsky, S., N. Oreskes, J. S. Risbey, B. R. Newell, and M. Smithson. 2015. "Seepage: Climate Change Denial and Its Effect on the Scientific Community." *Global Environmental Change* 33: 1–13.
- Liu, X., Z.-Y. Yin, X. Shao, and N. Qin. 2006. "Temporal Trends and Variability of Daily Maximum and Minimum, Extreme Temperature Events, and Growing Season Length Over the Eastern and Central Tibetan Plateau During 1961–2003." *Journal of Geophysical Research: Atmospheres* 111 (D19): D19109. doi:10.1029/2005JD006915.
- Marbà, N., G. Jordà, S. Agustí, C. Girard, and C. M. Duarte. 2015. "Footprints of Climate Change on Mediterranean Sea Biota." *Frontiers in Marine Science* 2: 56.
- Mariotti, A., Y. Pan, N. Zeng, and A. Alessandri. 2015. "Long-term Climate Change in the Mediterranean Region in the Midst of Decadal Variability." *Climate Dynamics* 44 (5-6): 1437–1456.
- Meehl, G. A., A. Hu, B. D. Santer, and S.-P. Xie. 2016. "Contribution of the Interdecadal Pacific Oscillation to Twentieth-century Global Surface Temperature Trends." *Nature Climate Change* 6 (11): 1005.
- Meinshausen, M., N. Meinshausen, W. Hare, S. C. Raper, K. Frieler, R. Knutti, D. J. Frame, and M. R. Allen. 2009. "Greenhouse-gas Emission Targets for Limiting Global Warming to 2 c." *Nature* 458 (7242): 1158.
- NASA-NEX. 2014. *Space Apps Challenge 2014*. https://nex.nasa.gov/nex/projects/1348/wiki/general_data_access_and_apis/.

- NOAA-WOCE. 2002. *Ocean Boundary Definitions*. https://www.nodc.noaa.gov/woce/woce_v3/wocedata_1/woce-uo/summary/sumindx.htm.
- Otto, F. E., G. J. van Oldenborgh, J. Eden, P. A. Stott, D. J. Karoly, and M. R. Allen. 2016. "The Attribution Question." *Nature Climate Change* 6 (9): 813.
- Pearson, R. G. 2007. "Species Distribution Modeling for Conservation Educators and Practitioners." *Synthesis. American Museum of Natural History* 50: 54–89.
- Pickett, E. J., D. L. Thomson, T. A. Li, and S. Xing. 2015. "Jensens Inequality and the Impact of Short-term Environmental Variability on Long-term Population Growth Rates." *PLoS One* 10 (9): e0136072.
- Rabiner, L. R., and B. Gold. 1975. *Theory and Application of Digital Signal Processing*, 777 p. Englewood Cliffs, NJ: Prentice-Hall.
- Ready, J., K. Kaschner, A. B. South, P. D. Eastwood, T. Rees, J. Rius, E. Agbayani, S. Kullander, and R. Froese. 2010. "Predicting the Distributions of Marine Organisms at the Global Scale." *Ecological Modelling* 221 (3): 467–478.
- Ruti, P. M., S. Somot, F. Giorgi, C. Dubois, E. Flaounas, A. Obermann, A. Dell'Aquila, G. Pisacane, A. Harzallah, E. Lombardi, et al. 2016. "Med-Cordex Initiative for Mediterranean Climate Studies." *Bulletin of the American Meteorological Society* 97 (7): 1187–1208.
- Sauerborn, R., and K. Ebi. 2012. "Climate Change and Natural Disasters – Integrating Science and Practice to Protect Health." *Global Health Action* 5 (1): 19295.
- Scheffer, M., S. Carpenter, J. A. Foley, C. Folke, and B. Walker. 2001. "Catastrophic Shifts in Ecosystems." *Nature* 413 (6856): 591.
- Schine, C. M., G. van Dijken, and K. R. Arrigo. 2016. "Spatial Analysis of Trends in Primary Production and Relationship with Large-scale Climate Variability in the Ross Sea, Antarctica (1997–2013)." *Journal of Geophysical Research: Oceans* 121 (1): 368–386.
- Schleussner, C.-F., J. F. Donges, R. V. Donner, and H. J. Schellnhuber. 2016. "Armed-conflict Risks Enhanced by Climate-related Disasters in Ethnically Fractionalized Countries." *Proceedings of the National Academy of Sciences* 113 (33): 9216–9221.
- Schrier, G., E. Besselaar, A. Klein Tank, and G. Verver. 2013. "Monitoring European Average Temperature Based on the E-obs Gridded Data Set." *Journal of Geophysical Research: Atmospheres* 118 (11): 5120–5135.
- Secretariat of the Convention on Biological Diversity. 2009. *Review of the Literature on the Links Between Biodiversity and Climate Change: Impacts, Adaptation, and Mitigation*. No. 42 in 1. UNEP/Earthprint.
- Shaltout, M., and A. Omstedt. 2014. "Recent Sea Surface Temperature Trends and Future Scenarios for the Mediterranean Sea." *Oceanologia* 56 (3): 411–443.
- Thrasher, B., and R. Nemani. 2015. *NASA Earth Exchange Global Daily Downscaled Projections (NEX-GDDP)*. https://nex.nasa.gov/static/media/other/NEXGDDP_Tech_Note_v1_08June2015.pdf.
- Thrush, S. F., J. E. Hewitt, P. K. Dayton, G. Coco, A. M. Lohrer, A. Norkko, J. Norkko, and M. Chiantore. 2009. "Forecasting the Limits of Resilience: Integrating Empirical Research With Theory." *Proceedings of the Royal Society of London B: Biological Sciences*. doi:10.1098/rspb.2009.0661.
- Uhe, P., F. Otto, K. Haustein, G. Oldenborgh, A. King, D. Wallom, M. Allen, and H. Cullen. 2016. "Comparison of Methods: Attributing the 2014 Record European Temperatures to Human Influences." *Geophysical Research Letters* 43 (16): 8685–8693.